

A Functional Block Decomposition Method for Automatic Op-Amp Design

Inga Abel, Maximilian Neuner, Helmut Graeb

Technical University of Munich, Arcisstr. 21, 80333 Munich

Abstract

This paper presents a method to decompose an op-amp into its functional blocks. The method is able to recognize functional blocks on a high level of abstraction as loads or amplification stages which have a large set of possible structural implementations. The paper presents a hierarchical library of functional blocks. With every hierarchy level, the structural representation of the functional blocks becomes more variable while its function emerges. We use the hierarchical order to automatically compute the functional decomposition of an op-amp given as a flat netlist. Experimental results illustrate the method. The functional block decomposition enables a comprehensive formalization of design knowledge for computer-aided design of op-amps. Applications to circuit sizing and structural synthesis of op-amps are presented.

Keywords: Analog design automation, CMOS, operational amplifiers, structure analysis

1. Introduction

Operational amplifiers are the fundamental building blocks of analog/mixed-signal circuits. They mean to analog design, as some say, what inverters mean

Email addresses: inga.abel@tum.de (Inga Abel), maximilian.neuner@tum.de (Maximilian Neuner), helmut.graeb@tum.de (Helmut Graeb)

This document is the results of the research project “Verification and synthesis of structural properties of analog/mixed-signal circuits by Constraint Programming exemplified by ESD and level shifter circuits” (GR 1190/6-1) funded by the German Research Foundation (DFG).

to digital design. While inverters and the complete library of cells for digital circuits are designed almost fully automatically, op-amps are still designed mostly manual till now. This work presents a new approach to the old, but yet unsolved problem of a complete structural and functional representation of op-amps. As confirmed in [1], op-amp stage recognition is a hard task. To tackle this problem, a new hierarchical representation of functional blocks in op-amps is developed in this paper. The method achieves a complete recognition of all stages in an op-amp, their loads, transconductances and biases. The formalized computer-oriented description of the op-amp structure allows a development of new approaches on major parts on analog design automation (e.g., sizing [2], structural synthesis [3]).

Many types of structural libraries were invented to automate the analog design process. They consist of whole topologies of basic analog circuits [4, 5, 6], predefined modules of, e.g., amplification stages or bias circuits having a certain transistor structure [7], or basic building blocks being either single devices with additional self connections as in [8, 9] or transistor structures as, e.g., current mirrors, differential pairs [10, 11, 12, 13]. The libraries were developed for different purposes. Some are used for topology synthesis [5, 8, 9, 12, 13, 6]. Other were developed to generate constraints for sizing and layout [11] or to synthesize layouts [7].

The libraries come with disadvantages. As there exist thousands of topology variants for op-amps, libraries containing structural defined topologies or modules as in [4, 5, 7, 6] do not support all variants. Adding topologies or modules to the libraries often comes with a high set-up effort. Basic building block libraries, e.g., [8, 9, 12, 13, 11] comprise topology variations. However, used for circuit synthesis, they include impractical and redundant topologies in the process taking up unnecessary computation time. When they are used for sizing and layout generation not all necessary constraints are generated. The methods, e.g. [11], are not able to recognize the load of a first stage, making the usage of other methods necessary [14]. To include more building blocks being important for op-amp design in basic libraries, attempts were made using un-

35 supervised learning algorithms [15, 16]. However, these methods are still fragile and might not recognize all building blocks correctly.

In this paper, a method is presented which tackles the described disadvantages. It fills in the gap between libraries based on basic building blocks [10, 11, 12, 13] and libraries containing whole topologies [5, 4]. We achieve this
40 by capturing all building blocks the full way up to a complete op-amp. In the frequently cited papers [10, 11], the so-called sizing rules method systematically captured the structures and constraints from differential pairs and current mirrors up to a differential stage. This work additionally captures the load, transconductance and bias of amplification stages as well as the amplification
45 stages themselves and their bias. A new approach on describing building blocks in op-amps is developed, giving them a well-defined functional and structural description. While the structure of a current mirror was relatively easy to establish, capturing the structure of loads, biases and amplification stages is much more complicated. In particular, while the function of these building blocks is
50 well known they are implemented by a large variety of structures.

With the new method on formalizing existing structural knowledge of op-amps presented in this paper, new approaches to sizing and structural synthesis of op-amps are developed (Sec. 9, detailed information [2, 3]). Due to the complete recognition of relevant structures in op-amps, the new methods are
55 able to capture op-amp design knowledge presented in a large number of design books, e.g., [17, 18, 19, 20, 21] to a new extent of completeness using a new systematic presentation making it usable for computer-aided op-amp design. The design methods are positioned between classical design methods with more or less fixed design plans [22, 23, 24, 25, 4, 26], which have to be set up for each
60 new op-amp, and simulation-based numerical optimization approaches [27, 28, 29, 14, 30, 31, 32], which need a CAD tool setup and value seeding for each netlist. It is also positioned between optimization-based structural synthesis approaches [12, 33, 34, 13, 8] that create a large number of variants some of them being impractical or redundant, and approaches without involvement of
65 optimization that investigate only a very small number of variants [35, 5].

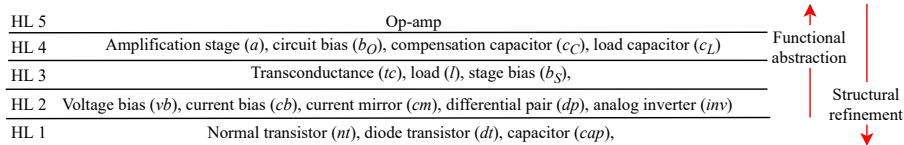


Figure 1: Hierarchical library of functional blocks in op-amps

The remainder of the paper is organized as follows: Sec. 2 gives a general overview of functional blocks in op-amps. Detailed explanations of the individual functional block are given in Secs. 3 - 6. The algorithms to recognize the blocks in an op-amp are presented in Sec. 7. In Sec. 8, we discuss the corresponding experimental results. Sec. 9 shows the application of the functional block decomposition method on circuit synthesis and sizing. A conclusion and an outlook on future work are presented in Secs. 10.

2. Functional Blocks in Op-Amps

An op-amp can be hierarchically decomposed into functional blocks. Fig. 1 shows this decomposition. Starting with one functional block at the highest hierarchy level (HL 5), the number of functional blocks per level increases till on the lowest level (HL 1) every device of the circuit forms a functional block of its own. On HL 1, every functional block is represented by one uniquely definable device composition. However, this level does not give any information about the functional task a device fulfills in the op-amp, e.g. amplification, stabilization, biasing. This functional assignment is given at HL 3 and HL 4. At these levels, the function of every functional block is uniquely definable. However, the structural description is not unique as e.g. different types of amplification stages exist. On HL 2, neither the structural nor the functional definition of the functional blocks is unique. However, their structural complexity is less than those of the functional blocks of HL 3 and HL 4.

Fig. 2 shows as an example the functional blocks in a symmetrical op-amp. For HL 1 and HL 2 (Fig 2a), all functional blocks of the same type have similar device compositions. This is different for HL 3 and HL 4 (Fig 2b). The

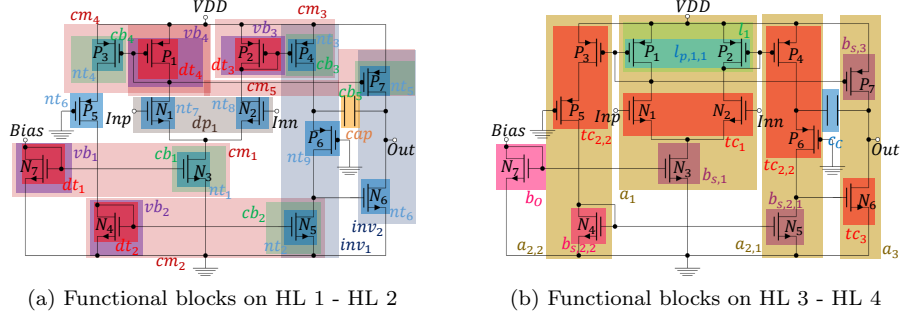


Figure 2: Symmetrical op-Amp with high PSRR [18] (Definitions of abbreviations in Fig. 1)

90 composition of the first stage a_1 differs highly from the composition of the other stages. On HL 1, HL 3, and HL 4, all devices can only be part of one functional block on a level. N_5 is a normal transistor nt_2 on level 1, a stage bias $b_{2,1}$ on level 3 and part of an amplification stage $a_{2,1}$ on level 4. On HL 2, a device can be part of more than one functional block. On this level, N_5 is a current bias
 95 cb_2 , part of a current mirror cm_2 and part of an analog inverter inv_1 .

We define the set of functional blocks \mathcal{X} in an op-amp as:

$$\mathcal{X} = \{x_k | k = 1, 2, \dots, |\mathcal{X}|\} \quad (1)$$

A functional block x_k in a circuit consists either of a basic device d_k of type $d_k.type \in \{t, c\}$, where t is referring to transistors and c to capacitors, or of other functional blocks $x_{k,1}, \dots, x_{k,n}$ of individual types $x_{k,l}.type \in \{dt, nt, cap, vb, cb, cm, dp, inv, g, l, b, a, c_L, c_C\}$ (see Fig. 1):

$$\forall x_k \in \mathcal{X} (x_k = \{d_k\} \vee x_k = \{x_{k,1}, \dots, x_{k,n}\}) \quad (2)$$

The subset $\mathcal{X}_j \subseteq \mathcal{X}$ contains all functional blocks $x_k \in \mathcal{X}$ with $x_k.type = j$.

To describe the connections between functional blocks, every functional block x_k is assigned a set of pins P_{x_k} , which are connected to the nets of the circuit:

$$P_{x_k} = \{x_k.p_l | l = 1, 2, \dots, |P_{x_k}|\} \quad (3)$$

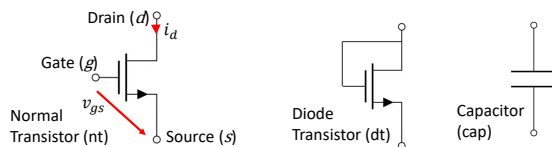


Figure 3: Functional blocks on level 1

As all functional blocks consist at the end of devices, the pins P_{x_k} of a functional block x_k refer to certain device pins.

A connection of two functional blocks x_k, x_l over any net with the pins $x_k.p_y, x_l.p_z$ is described by:

$$x_k.p_y \leftrightarrow x_l.p_z \quad (4)$$

To describe that two pins $x_k.p_y, x_l.p_z$ are not allowed to be connected by any net, the following notation is used:

$$x_k.p_y \leftrightarrow\leftrightarrow x_l.p_z \quad (5)$$

$x_k.\Phi$ denotes the substrate type of a functional block x_k , with following naming convention:

$$x_k.\Phi \in \{\Phi_n, \Phi_p, \Phi_u\}, \text{ for n-, p-, or mixed-doping} \quad (6)$$

A functional block x_k has mixed-doping if it consists of transistors with different doping. 100

In the following, structural and functional definitions will be given for all functional block types in Fig. 1. Please note that all examples shown for NMOS transistors, hold analogously for PMOS transistors.

3. Functional Blocks on Hierarchy Level 1

Fig. 3 shows three different device level functional blocks. In addition to capacitors, we define and use two different functional block types for transistors: 105

3.1. Normal Transistor

Function: A normal transistor nt_k establishes a relation between the the voltage potential v_g at the gate of the transistor and the current at the drain i_d of the transistor. Either v_g or i_d is the control factor.

Structure: A normal transistor nt_k is a transistor d_k without any self connections.

$$\begin{aligned} x_k = \{d_k\} \wedge d_k.type = t \wedge d_k.d \leftrightarrow d_k.s \wedge d_k.d \leftrightarrow d_k.g \\ \wedge d_k.g \leftrightarrow d_k.s \Leftrightarrow x_k.type = nt \end{aligned} \quad (7)$$

3.2. Diode Transistor

Function: A diode transistor dt converts its drain-source current i_d into a stable gate-source voltage v_{gs} .

Structure: A diode transistor dt_k is a transistor d_k , whose drain $d_k.d$ is connected to its gate $d_k.g$:

$$x_k = \{d_k\} \wedge d_k.type = t \wedge d_k.d \leftrightarrow d_k.g \wedge d_k.d \leftrightarrow d_k.s \Leftrightarrow x_k.type = dt \quad (8)$$

4. Functional Blocks on Hierarchy Level 2

The majority of the functional blocks on HL 2 consist of transistor stacks. Typical transistor stacks are shown in Fig. 4, 5. A transistor stack ts_k is a set of 1-3 transistors having the same doping and a drain-source connection i.e., the drain of a lower transistor in the stack $x_{k,m}.d$ is connected with the source of the next higher transistor $x_{k,m+1}.s$. Higher transistor gates are not allowed to be connected to drains of lower transistors. Drains of higher transistors are not allowed to be connected to lower transistor sources.

$$\begin{aligned} x_k = \{x_{k,1}, \dots, x_{k,n} | n = |x_k| \wedge n \leq 3\} \wedge x_k \subset (\mathcal{X}_{nt} \cup \mathcal{X}_{dt}) \wedge x_{k,m}.d \leftrightarrow x_{k,m+1}.s \\ \wedge x_{k,m}.\Phi = x_{k,m+1}.\Phi \wedge x_{k,m+1}.g \leftrightarrow x_{k,m}.d \wedge x_{k,m+1}.d \leftrightarrow x_{k,m}.s \\ \Leftrightarrow x_k.type = ts \end{aligned} \quad (9)$$

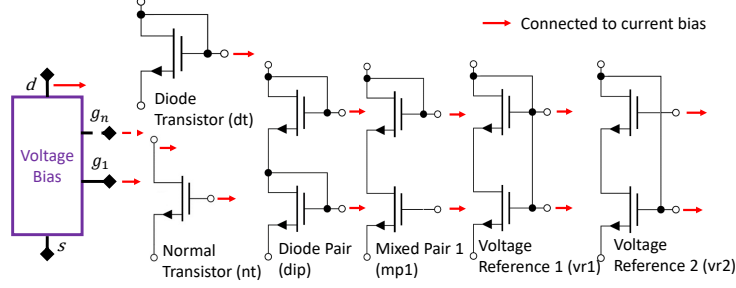


Figure 4: Voltage bias and variants with stacks of 1 or 2 transistors (dashed lines: optional pins and functional blocks)

115 The usual number of transistors in a stack is 1-2. For the pins in a transistor stack, the following naming convention will be used. The source not connected to any drain in the stack $ts_k.s_1$ is the source $ts_k.s$ of the transistor stack. The drain not connected to any source of the stack $ts_k.d_n$ is the drain $ts_k.d$ of the transistor stack. If all drains or sources of the stack must be considered,
 120 numbering will be used. The definition of the transistor stack is in the following used to describe the functional blocks in detail.

4.1. Voltage Bias

Function: A voltage bias vb_k converts its drain current i_d into a stable gate-source voltage v_{gs} applied to a gate of a current bias.

Structure: A voltage bias vb_k (Fig. 4) consists of a transistor stack $x_k, x_k.type = ts$, with the gates of its devices $x_k.g_l$ connected to gates of a current bias cb_v with same doping as vb_k . Additionally, the drain of the stack $x_k.d = x_{k,n}.d$ must be connected to a gate $cb_v.g_m$ of cb_v . For every gate $x_k.g_j$ in the stack, exactly one gate-drain connection with another transistor $x_y \in (\mathcal{X}_{nt} \cup \mathcal{X}_{dt})$ of same doping exists. This transistor x_y must be part of a voltage or current bias $x_z \in (\mathcal{X}_{vb} \cup \mathcal{X}_{cb})$ but not necessarily of vb_k or cb_v itself.

$$\begin{aligned}
 x_k &= \{x_{k,1}, \dots, x_{k,n} | n = |x_k|\} \wedge x_k.type = ts \wedge \exists_{cb_v} [cb_v.\Phi = x_k.\Phi \wedge x_{k,n}.d \\
 &\leftrightarrow cb_v.g_m \wedge \forall_{x_k.g_l} [x_k.g_l \leftrightarrow cb_v.g_l] \wedge \forall_{x_k.g_j} [\exists!_{x_y \in (\mathcal{X}_{nt} \cup \mathcal{X}_{dt})} [(x_y.\Phi = x_k.\Phi \quad (10) \\
 &\wedge x_y.d \leftrightarrow x_k.g_j) \longleftrightarrow \exists!_{x_z \in (\mathcal{X}_{vb} \cup \mathcal{X}_{cb})} x_y \in x_z] \leftrightarrow x_k.type = vb
 \end{aligned}$$

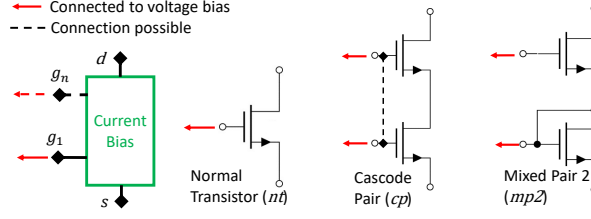


Figure 5: Current bias and variants with stacks of 1 or 2 transistors (dashed lines: optional)

125 4.2. Current Bias

Function: A current bias cb_k converts the voltage potential v_g applied at its gates into a drain current i_d .

Structure: A current bias cb_k (Fig. 5) consists typically of a stack of normal transistors, which might have a gate connection. In rare cases, the normal transistor at the bottom is exchanged by a diode transistor. The gates of a current bias $cb_k.g_l$ are connected to a gate or the upper drain of a voltage bias ($vb_v.g_l \vee vb_v.d$). The voltage bias must have the same doping. The drain of the upper transistor of a current bias $cb_{k,n}.d = cb_k.d$ must not be connected to any gate of a voltage bias $vb_y.g_z$ with same doping.

$$\begin{aligned}
 x_k = \{x_{k,1}, \dots, x_{k,n} | n = |x_k|\} \wedge x_k.type = ts \wedge \exists_{vb_v} [vb_v.\Phi = x_k.\Phi \wedge \forall_{x_k.g_l} [x_k.g_l \\
 \leftrightarrow (vb_v.g_l \vee vb_v.d)] \wedge \nexists_{vb_y} [vb_y.\Phi = x_k.\Phi \wedge x_{k,n}.d \leftrightarrow vb_y.g_z]] \Leftrightarrow x_k.type = cb
 \end{aligned}
 \tag{11}$$

4.3. Current Mirror

Function: A current mirror cm_k provides a current by the current bias, specified by the devices sizes and the current of the voltage bias.

Structure: Fig. 6 shows the structural definition of a current mirror and examples. To form a current mirror cm_k , voltage bias vb_k and current bias cb_k must have equal doping and a source connection. The gates of the voltage bias $vb_k.g_l$ must be connected to the gates $cb_k.g_l$ of the current bias. The uppermost drain of the voltage bias $vb_k.d$ must be connected to a gate of the current bias $cb_k.g_m$. All gates of the voltage bias $vb_k.g_j$ with exception of the upper most

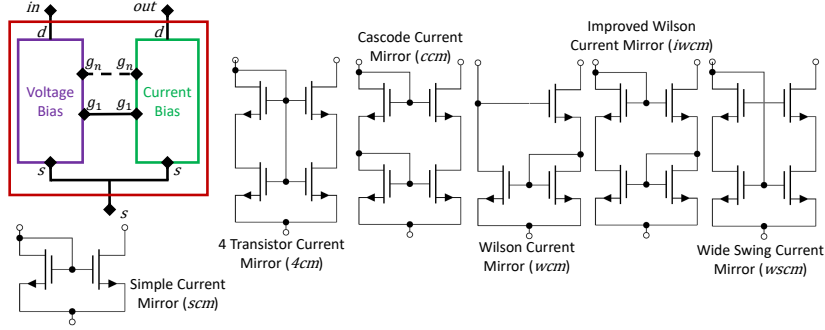


Figure 6: Current mirror and examples (dashed lines: optional)

one $vb_k.g|_{vb_k}$ must have a connection to a drain of either voltage or current bias $x_y.d_z|_{x_y \in \{vb_k, cb_k\}}$.

$$\begin{aligned}
 x_k &= \{vb_k, cb_k\} \wedge vb_k.\Phi = cb_k.\Phi \wedge vb_k.s \leftrightarrow cb_k.s \wedge (vb_k.g_l \leftrightarrow cb_k.g_l)|_{l \leq |vb_k|} \\
 &\wedge \exists cb_k.g_m [cb_k.g_m \leftrightarrow vb_k.d] \wedge \forall vb_k.g_j \in P_{vb_k} \setminus \{vb_k.g|_{vb_k}\} [\exists! x_y.d_z \in P_{x_y} |_{x_y \in \{vb_k, cb_k\}} \\
 &[vb_k.g_j \leftrightarrow x_y.d_z]] \Leftrightarrow x_k.type = cm
 \end{aligned} \tag{12}$$

4.4. Differential Pair

Function: A differential pair dp_k converts the voltage potentials at the gates of its two input transistor into amplified drain currents. Equal voltages lead to equal drain currents. Depending on the structure, higher amplification gains can be obtained. Cascode versions with four transistors have a higher amplification gain than a simple version with two transistors.

Structure: Fig. 7 shows the structure of a differential pair. The basic structure is the simple differential pair, which can also stand alone.

A *simple differential pair* dp_k consist of two normal transistors $nt_{k,1}, nt_{k,2}$ connected only at their sources. This common source $dp_k.s$ must be connected to a current bias drain $cb_l.d$. The two normal transistors and the current bias

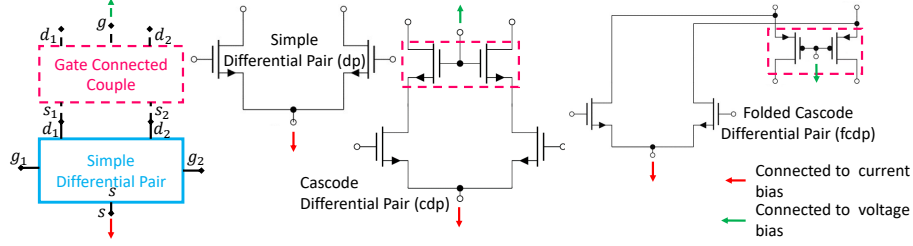


Figure 7: Differential pair and examples (dashed lines: optional)

must have equal doping.

$$\begin{aligned}
 x_k &= \{nt_{k,1}, nt_{k,2}\} \wedge nt_{k,1}.\Phi = nt_{k,2}.\Phi \wedge nt_{k,1}.s \leftrightarrow nt_{k,2}.s \wedge nt_{k,1}.d/g \\
 &\Leftrightarrow nt_{k,2}.d/g \wedge \exists_{cb_l} [nt_{k,1}.s \leftrightarrow cb_l.d \wedge nt_{k,1}.\Phi = cb_l.\Phi] \Leftrightarrow x_k.type = dp
 \end{aligned} \tag{13}$$

For the cascode version of the differential pair vdp_k , a simple differential pair dp_k is connected with its drains to the sources of a *gate connected couple* gcc_k . These are two normal transistor with same doping connected at their gates:

$$\begin{aligned}
 x_k &= \{nt_{k,1}, nt_{k,2}\} \wedge nt_{k,1}.\Phi = nt_{k,2}.\Phi \wedge nt_{k,1}.g \leftrightarrow nt_{k,2}.g \\
 &\wedge nt_{k,1}.d/s \Leftrightarrow nt_{k,2}.d/s \Leftrightarrow x_k.type = gcc
 \end{aligned} \tag{14}$$

The structural definition of the *cascode version of the differential pair* vdp_k is:

$$\begin{aligned}
 x_k &= \{dp_k, gcc_k\} \wedge (dp_k.d_l \leftrightarrow gcc_k.s_l) |_{l=1,2} \wedge dp_k.s/g_{1,2} \Leftrightarrow gcc_k.g/d_{1,2} \\
 &\Leftrightarrow x_k.type = vdp
 \end{aligned} \tag{15}$$

Two types of cascode variants exist having different doping characteristics. In the *folded cascode differential pair* $fcdp_k$, dp_k and gcc_k have opposite doping:

$$vdp_k = \{dp_k, gcc_k\} \wedge dp_k.\Phi \neq gcc_k.\Phi \Leftrightarrow vdp_k.type = fcdp \tag{16}$$

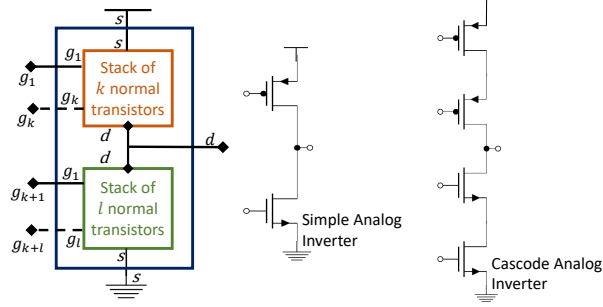


Figure 8: Analog inverter and examples (dashed lines: optional)

In the *cascode differential pair* cdp_k , they have equal doping:

$$vdp_k = \{dp_k, gcc_k\} \wedge dp_k.\Phi = gcc_k.\Phi \Leftrightarrow vdp_k.type = cdp \quad (17)$$

4.5. Analog Inverter

140 *Function:* An analog inverter inverts and amplifies an input voltage applied at one of its gates.

Structure: An analog inverter inv_k (Fig. 8) consists of two normal transistor stacks $ts_{k,1}, ts_{k,2}$ differing in doping. The stacks are connected at their drains $ts_{k,1}.d, ts_{k,2}.d$. The two sources $ts_{k,1}.s, ts_{k,2}.s$ are connected to the supply voltage rail that corresponds to the doping type. Gate-gate, gate-drain and source-source connections between transistors are not allowed.

$$\begin{aligned} x_k &= \{ts_{k,1}, ts_{k,2}\} \wedge (ts_{k,1} \cup ts_{k,2}) \subset \mathcal{X}_{nt} \wedge ts_{k,1}.d \leftrightarrow ts_{k,2}.d \wedge ts_{k,1}.\Phi = \Phi_p \\ &\wedge ts_{k,2}.\Phi = \Phi_n \wedge ts_{k,1}.s \leftrightarrow VDD \wedge ts_{k,2}.s \leftrightarrow GND \\ &\wedge \forall_{nt_i, nt_j \in (ts_{k,1} \cup ts_{k,2})} [nt_i.g \leftrightarrow nt_j.g \wedge nt_i.d \leftrightarrow nt_j.d \wedge nt_i.s \leftrightarrow nt_j.s] \\ &\Leftrightarrow x_k.type = inv \end{aligned} \quad (18)$$

4.6. Multiple Assignments of Transistors to Functional Blocks

Hierarchy level 2 is the only level which allows transistors to be part of more than one functional block. An example are current mirrors. According

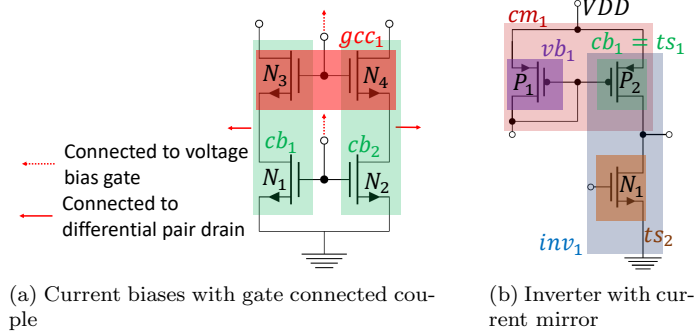


Figure 9: Relevant multiple assignments

145 to (12), every transistor in a current mirror $t_k \in cm_k$ is at the same time part of a voltage or current bias $t_k \in (vb_k \cup cb_k)$. We distinguish between relevant, irrelevant and false multiple assignments.

Relevant multiple assignments are circuitry-wise correct and obtain additional information needed to find other functional blocks. These are the above mentioned double assignments in current mirrors, different current mirrors with the same voltage bias but different current biases forming a current mirror bench, and the two cases shown in Fig. 9. Fig. 9a shows a gate connected couple (14) gcc_1 in two current biases cb_1, cb_2 . The gate connected couple must be part of a cascode version of a differential pair vdp_1 (15). The transistors 155 N_3, N_4 are therefore part of gcc_1, vdp_1 and cb_1 or cb_2 . Fig. 9b shows an analog inverter with a transistor stack $ts_1 = \{P_2\}$ that is also part of a current mirror cm_1 . Thus, P_2 is part of inv_1, cm_1 and the current bias cb_1 in cm_1 .

Irrelevant multiple assignments are circuitry-wise correct but do not obtain any additional information to the functional behavior as the functional blocks the transistor is in are of the same type. An example is a simple current mirror in a cascode current mirror (Fig. 10a). The simple current mirror does not obtain any additional information to the cascode current mirror. To avoid such irrelevant multiple assignments of transistors following rule is used:

$$\forall_{x_k \in \mathcal{X}_{min}} [\exists_{x_l \in \mathcal{X}} (x_k \subset x_l \wedge x_k.type = x_l.type)] \Leftrightarrow x_k \text{ is irrelevant} \quad (19)$$

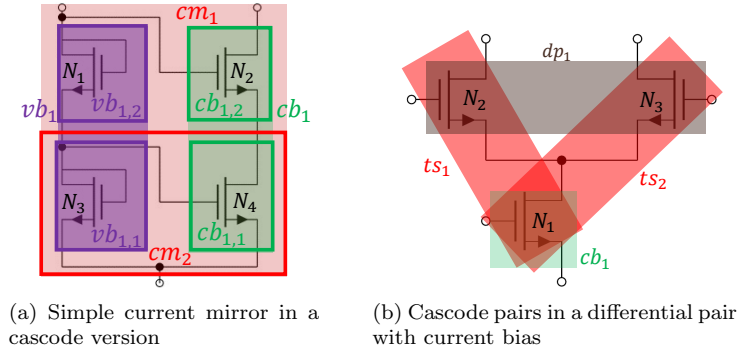


Figure 10: Irrelevant (a) and false (b) multiple assignments

\mathcal{X}_{min} contains all functional blocks which are potential irrelevant. These are all current mirrors, voltage and current biases.

160 *False multiple assignments* are circuitry-wise incorrect, e.g., two transistor stacks in a differential pair with current bias (Fig 8). With suitable transistors connected at the drain of the differential pair, these false transistor stacks might form analog inverters. By suppressing the recognition of these transistor stacks, the false recognition of analog inverters is omitted.

165 5. Functional Blocks on Hierarchy Level 3

On HL 3 are the functional block types that form the amplification stages (HL 4) of an op-amp, i.e., transconductance, load and stage bias.

5.1. Transconductance

Function: A transconductance converts a voltage potential applied at its gates into an (amplified) current.
170

Structure: Fig. 11 shows the structural definition of a transconductance tc_k as well as examples. Two different types of transconductance exist, non-inverting and inverting.

A *non-inverting transconductance* tc_{ninv} consists of 1 or 2 differential pairs.
175 We further define three different types having three different structures:

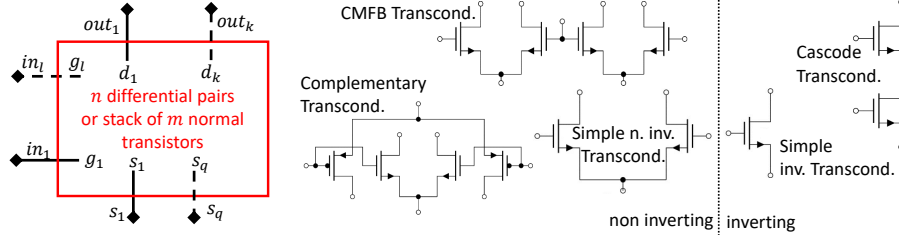


Figure 11: Transconductance (Transcond.) and examples (dashed lines: optional)

A *simple transconductance* tc_s is a transconductance consisting of one differential pair, having no gate connection to any other differential pair.

$$x_k = \{dp_k\} \wedge \nexists_{dp_l} (dp_k.g_y|_{y=1,2} \leftrightarrow dp_l.g_z|_{z=1,2}) \Leftrightarrow x_k.type = tc_s \quad (20)$$

A *complementary Transconductance* tc_c consists of two differential pairs with opposite doping and connected at both gates

$$x_k = \{dp_{k,1}, dp_{k,2}\} \wedge (dp_{k,1}.g_l \leftrightarrow dp_{k,2}.g_l)|_{l=1,2} \wedge dp_{k,1}.\Phi \neq dp_{k,2}.\Phi \quad (21)$$

$$\Leftrightarrow x_k.type = tc_c$$

A *common-mode feedback (CMFB) transconductance* tc_{CMFB} consists of two differential pairs with equal doping connected at one of the two gates:

$$x_k = \{dp_{k,1}, dp_{k,2}\} \wedge \exists!_{dp_{k,1}.g_m, dp_{k,2}.g_n} [dp_{k,1}.g_m \leftrightarrow dp_{k,2}.g_n] \quad (22)$$

$$\wedge dp_{k,1}.\Phi = dp_{k,2}.\Phi \Leftrightarrow x_k.type = tc_{CMFB}$$

A *inverting transconductance* tc_{inv} consists of a transistor stack ts_k of m normal transistors, with the source $ts_k.s$ connected to a supply voltage rail. No gate-gate and gate-drain connection of the transistors in the stack is allowed. The gate of the bottom transistor in the stack $ts_k.g_1$ is connected to the output of another transconductance $tc_v.out_p$ or to the output of a load $l_w.out_q$. The

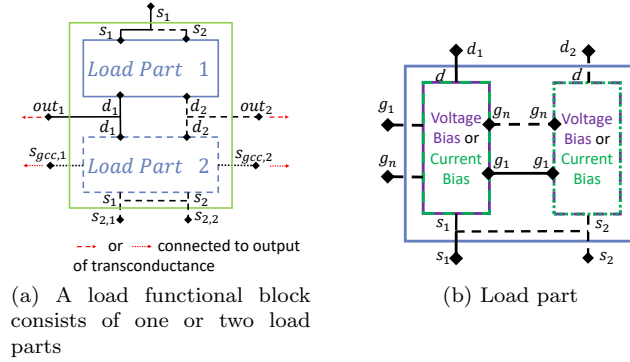


Figure 12: Load (dashed lines: optional)

drain of the stack $ts_k.d$ is connected to the output of a stage bias $b_{s,y}.out_z$.

$$\begin{aligned}
x_k = \{ts_k\} \wedge ts_k \in \mathcal{X}_{nt} \wedge \text{net}(ts_k.s) \in \mathcal{N}_{supply} \forall nt_i, nt_j \in ts_k (nt_i.g/d \leftrightarrow nt_j.g/d) \\
\wedge [\exists tc_v [tc_v.out_p \leftrightarrow ts_k.g_1] \vee \exists l_w [l_w.out_q \leftrightarrow ts_k.g_1]] \wedge \exists b_{s,y} [b_{s,y}.out_z \leftrightarrow ts_k.d] \\
\Leftrightarrow x_k.type = tc_{inv}
\end{aligned} \tag{23}$$

The definition of the load is given in the next section. The definition of the stage bias is given in Sec. 5.3.

5.2. Load

Function: A load converts a current into a voltage. It influences the gain generated by the connected transconductance.

Structure: Fig. 12 shows the structure of a load l_k . A load l_k consists of one or two load parts $l_{p,k,l}$ of type l_p . The parts are connected at their drains and have different substrate types. If a gate connected couple gcc_j is in one of the load parts, its sources $gcc_j.s_y$ are connected to the output of a transconductance tc_w of type tc_{inv} . Otherwise, if no gate connected-couple is in one of the load

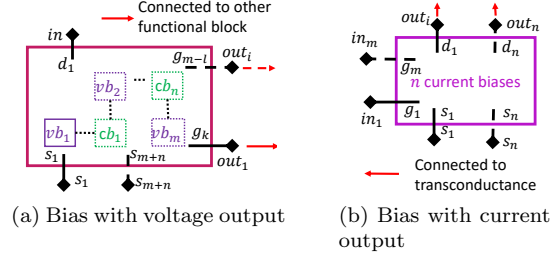


Figure 13: Different types of biases (dashed lines: optional)

parts, the outputs of the load $l_k.out_v$ are connected to $tc_w.out_v$.

$$\begin{aligned}
x_k = & \{x_{k,1}, \dots, x_{k,n} | n = |x_k| \wedge n \leq 2\} \wedge x_k \subseteq \mathcal{X}_{l_p} \wedge [n = 2 \rightarrow [x_{k,1}.\Phi \neq x_{k,2}.\Phi \\
& \wedge (x_{k,1}.d_l \leftrightarrow x_{k,2}.d_l) |_{l=1,2}] \wedge [\exists_{gcc_j \in x_k} [(gcc_j.s_y \leftrightarrow tc_z.out_y) |_{y=1,2,tc_z.type=tc_{ninv}}] \\
& \oplus (x_k.out_v \leftrightarrow tc_w.out_v) |_{v \leq |x_{k,1}|, tc_w.type=tc_{ninv}}] \Leftrightarrow x_k.type = l
\end{aligned} \tag{24}$$

A single load part $l_{p,k,l}$ consists of one or two transistor stacks, which have gate-gate connections. A transistor stack in a load part is either of type voltage or current bias. If no gate connected-couple is in the load part, the sources must be connected. The doping of the transistor stacks is equal.

$$\begin{aligned}
x_k = & \{x_{k,1}, \dots, x_{k,n} | n = |x_k| \wedge n \leq 2\} \wedge x_k \subset (\mathcal{X}_{vb} \cup \mathcal{X}_{cb}) \wedge (x_{k,1}.g_l \\
& \leftrightarrow x_{k,n}.g_l) |_{l \leq |x_{k,1}|} \wedge \exists_{gcc_l \in x_k} [x_{k,1}.s \leftrightarrow x_{k,n}.s] \wedge x_{k,1}.\Phi = x_{k,n}.\Phi \Leftrightarrow x_k.type = l_p
\end{aligned} \tag{25}$$

5.3. Stage Bias

Function: A stage bias b_s supplies a transconductance with defined currents.

Structure: A stage bias b_s is a subtype of the type bias b (Fig. 13). Two different types exist.

A *bias with voltage output* b_v consists of m voltage and n current biases with $m > n$. Its input $b_{v,k}.in$ is the drain of a voltage bias. The outputs $b_{v,k}.out_1, \dots, b_{v,k}.out_i$ are gates of voltage biases, which are connected to gates

of other functional blocks. All current biases in $b_{v,k}$ must have a drain-drain connection to a voltage bias with opposite doping and a gate-gate connection to a voltage bias with equal doping in x_k .

$$\begin{aligned}
x_k &= \{x_{k,1}, \dots, x_{k,l} | l = |x_k|\} \wedge \{x_{k,1}, \dots, x_{k,m}\} \subset \mathcal{X}_{vb} \wedge (l \neq m \rightarrow \\
&\{x_{k,l-m}, \dots, x_{k,l}\} \subset \mathcal{X}_{cb}) \wedge \exists_{vb_{k,i} \in x_k} [vb_{k,i}.g_j \leftrightarrow x_z.g_y | x_z \in \mathcal{X} \setminus x_k] \wedge \forall_{cb_{k,q} \in x_k} [cb_{k,q}.d \\
&\leftrightarrow vb_{k,v}.d \wedge vb_{k,v} \in x_k \wedge cb_{k,q}.\Phi \neq vb_{k,v}.\Phi \wedge (cb_{k,q}.g_s \leftrightarrow vb_{k,w}.g.s) |_{s \leq |cb_{k,q}|} \\
&\wedge vb_{k,w} \in x_k \wedge cb_{k,q}.\Phi = vb_{k,w}.\Phi] \Leftrightarrow x_k.type = b_v
\end{aligned} \tag{26}$$

A bias with voltage output $b_{v,k}$ is a stage bias, iff it consists of exactly one voltage bias vb_k , which is connected with its drain $vb_k.d$ to the output of a transconductance of type inverting:

$$b_{v,k} = \{vb_k\} \wedge \exists_{tc_i} [tc_i.type = tc_{inv} \wedge vb_k.d \leftrightarrow tc_i.out] \Leftrightarrow b_{v,k}.type = b_s \tag{27}$$

185 In all other cases, if a bias with voltage out consists of more than one voltage bias or if it is not connected with its input pin to a transconductance, it is the circuit bias b_O (Sec. 6.2)

A bias with current output b_c consist of n current biases. Its inputs $in_1, ..in_m$ are the gates of the current biases. The outputs out_1, \dots, out_n are the drains of the current biases, which must be connected to the source or output of a transconductance.

$$\begin{aligned}
x_k &= \{cb_{k,1}, \dots, cb_{k,n} | n = |x_k|\} \wedge x_k \subset \mathcal{X}_{cb} \wedge \forall_{cb_{k,l} \in x_k} [cb_{k,l}.d \\
&\leftrightarrow (tc_z.s |_{tc_z.type=tc_{inv}} \vee tc_z.out_y |_{tc_z.type=tc_{inv}})] \Leftrightarrow x_k.type = b_c
\end{aligned} \tag{28}$$

A bias with current output is always a stage bias:

$$\forall_{b_k \in \mathcal{X}_b} [b_k.type = b_c \rightarrow b_k.type = b_s] \tag{29}$$

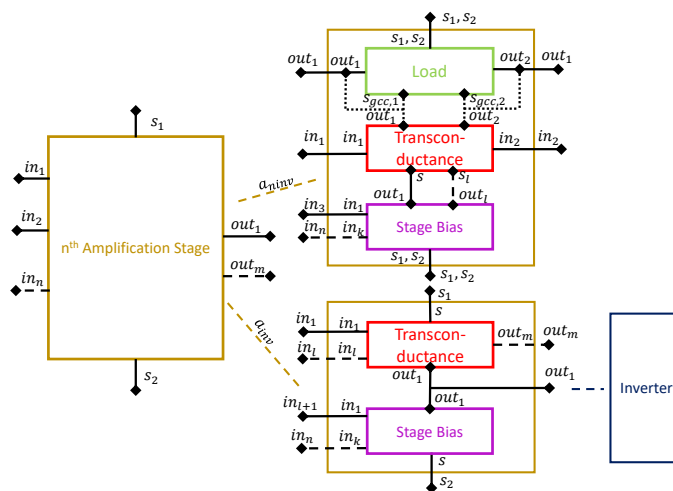


Figure 14: Amplification stage (dashed lines: optional)

6. Functional Blocks on Hierarchy Level 4

The functional block types on HL 4 are the amplification stage, the circuit
 190 bias, the compensation and load capacitor.

6.1. Amplification Stage

Function: Two functional types of amplification stage exist: the n^{th} amplification stage of an op-amp a_n and the common-mode feedback stage a_{CMFB} . The n^{th} amplification stage a_n amplifies the input signal for the n^{th} time. A
 195 common-mode feedback (CMFB) stage a_{CMFB} amplifies the output signals of a fully differential op-amp while comparing them to a reference voltage and feeds them back to the amplifier.

Structure: Fig. 14 shows the general composition of the amplification stages of an op-amp. Every amplification stage has at least two inputs and one output.
 200 It has a source connection to both supply voltage rail. Two structural types of amplification stages exist, non-inverting and inverting amplification stages. Non-inverting amplification stages are the first stage of an op-amp and the CMFB stage. Inverting stages form the further stages of an op-amp ($n \geq 2$). In the following, both types are described in detail.

A *non-inverting amplification stage* a_{ninv} consists of a transconductance tc_k , a load l_k and a stage bias $b_{s,k}$. The transconductance must be of type non-inverting and the stage bias must have a current output connected to the sources of the transconductance. The load outputs or the sources of a gate connected couple in the load must be connected to the outputs of the transconductance.

$$\begin{aligned}
x_k &= \{tc_k, l_k, b_{s,k}\} \wedge tc_k.type = tc_{ninv} \wedge b_{s,k}.type = b_c \wedge [\exists gcc_i \in l_k [(gcc_i.s_j \\
&\leftrightarrow tc_k.out_j) |_{j=1,2}] \oplus \forall l_k.out_v \in P_{l_k} [l_k.out_v \leftrightarrow tc_k.out_w]] \\
&\wedge (tc_k.sl \leftrightarrow b_{s,k}.out_l) |_{l \leq |tc_k|} \Leftrightarrow x_k.type = a_{ninv}
\end{aligned} \tag{30}$$

205 Non-inverting amplification stages are classified into three types: simple first stage a_s , complementary first stage a_c , and CMFB stage a_{CMFB} . The types differ in the transconductance types and the doping characteristics of its functional blocks.

A *simple first stage* a_s has a transconductance of type tc_s . The transconductance and the stage bias have the same substrate type, while the load has either the opposite doping or mixed doping.

$$\begin{aligned}
a_{ninv} &= \{tc_k, l_k, b_{s,k}\} \wedge tc_k.type = tc_s \wedge (tc_k.\Phi = b_{s,k}.\Phi) \in \{\Phi_n, \Phi_p\} \\
&\wedge tc_k.\Phi \neq l_k.\Phi \Leftrightarrow a_{ninv}.type = a_s
\end{aligned} \tag{31}$$

A *complementary first stage* a_c has a transconductance of type tc_c . Transconductance, load and stage bias have all mixed doping.

$$\begin{aligned}
a_{ninv} &= \{tc_k, l_k, b_{s,k}\} \wedge tc_k.type = tc_c \wedge tc_k.\Phi = b_{s,k}.\Phi = l_k.\Phi = \Phi_u \\
&\Leftrightarrow a_{ninv}.type = a_c
\end{aligned} \tag{32}$$

A *common-mode feedback stage* a_{CMFB} has a transconductance of type tc_{CMFB} . Transconductance and stage bias have the same substrate type, while

the load has opposite doping.

$$\begin{aligned}
a_{inv} &= \{tc_k, l_k, b_{s,k}\} \wedge tc_k.type = tc_{CMFB} \wedge (tc_k.\Phi = b_{s,k}.\Phi) \in \{\Phi_n, \Phi_p\} \\
&\wedge tc_k.\Phi \neq l_k.\Phi|_{l_k.\Phi \in \{\Phi_n, \Phi_p\}} \Leftrightarrow a_{inv}.type = a_{CMFB}
\end{aligned} \tag{33}$$

A *inverting amplification stage* a_{inv} consists of a transconductance tc_k and a stage bias $b_{s,k}$ with opposite doping connected at their outputs. The transconductance must be of type inverting. The stage bias consists either of one voltage bias or one current bias.

$$\begin{aligned}
a_k &= \{tc_k, b_{s,k}\} \wedge tc_k.type = tc_{inv} \wedge b_{s,k}.type \in \{b_c, b_v\} \wedge |b_{s,k}| = 1 \\
&\wedge tc_k.out_1 \leftrightarrow b_{s,k}.out_1 \wedge tc_k.\Phi \neq b_{s,k}.\Phi \Leftrightarrow a_k.type = a_{inv}
\end{aligned} \tag{34}$$

Note, that all inverting stages can occur twice in an op-amp, e.g., two second stages. It appears when the op-amp is fully differential or a symmetrical op-amp (Fig. 2, with $a_{2,1}, a_{2,2}$).

Differentiating between an inverting stage with a stage bias with current output and an inverting stage with a stage bias with voltage output allows to give a more precise definition of inverting amplification stages:

A *inverting stage with stage bias with current output* a_{inv_c} must also fulfill the type definition of an analog inverter to be a valid inverting amplification stage:

$$a_{inv,k} = \{tc_{inv,k}, b_{s,k}\} \wedge b_{s,k}.type = b_c \wedge a_{inv,k}.type = inv \Leftrightarrow a_{inv,k}.type = a_{inv_c} \tag{35}$$

Note, that not all analog inverters are inverting stages, as the constraints for a transconductance (23) and stage bias (28) must hold.

A *inverting stage with stage bias with voltage output* a_{inv_v} only occurs in symmetrical OTAs, which are op-amps with a characteristic first stage and two second stages (Fig. 2). The first stage a_1 must be a simple first stage a_s having a load consisting of two voltage biases $vb_{l,1}, vb_{l,2}$ with same doping. Both voltage

biases must have a gate-gate connection to a transconductance in a second stage of type a_{inv} . One second stage a_z must be of type a_{inv_c} . The other second stage a_y must have a voltage bias as stage bias, which has a gate-gate connection to the stage bias of a_z :

$$\begin{aligned}
a_{inv,k} = & \{tc_{inv,k}, b_{s,k}\} \wedge b_{s,k}.type = b_v \wedge \exists_{a_1} [a_1.type = a_s \\
& \wedge \exists_{l_1 \in a_1} [|l_1| = 1 \wedge \exists_{l_{1,1} \in l_1} [\{vb_{l_{1,1}}, vb_{l_{1,2}}\} \subseteq l_{1,1} \wedge (vb_{l_{1,m}}.g_1 \leftrightarrow tc_{inv,k}.in_1 \\
& \wedge vb_{l_{1,n}}.g_1 \leftrightarrow a_i.in_1) |_{(m=1 \wedge n=2) \vee (m=2 \wedge n=1)} \wedge a_i.type = a_{inv_c} \\
& \wedge (b_{s,k}.out_v \leftrightarrow b_i.in_v |_{b_i \in a_i})]]] \Leftrightarrow a_{inv,k}.type = a_{inv_v}
\end{aligned} \tag{36}$$

6.2. Circuit Bias

Function: The circuit bias b_O supplies all functional blocks of type amplification stage a with voltages specified by b_O .

Structure: The circuit bias b_O has the structure of a bias with voltage output (26) (Fig. 13a). It contains all current biases and voltage biases not part of an amplification stage.

$$\begin{aligned}
x_k = & \{x_{k,1}, \dots, x_{k,n} | n = |x_k|\} \wedge x_k = [(\mathcal{X}_{vb} \cup \mathcal{X}_{cb}) \setminus \mathcal{X}_a] \wedge x_k.type = b_v \\
& \Leftrightarrow x_k.type = b_O
\end{aligned} \tag{37}$$

220 6.3. Compensation Capacitor

Function: A compensation capacitor $c_{C,k}$ increases the stability of an op-amp.

Structure: A compensation capacitor $c_{C,k}$ is connected between the outputs of two different amplification stages a_j, a_v :

$$x_k = \{cap_k\} \wedge [cap_k.p_1 \leftrightarrow a_j.out_i \wedge cap_k.p_2 \leftrightarrow a_v.out_w] |_{a_j \neq a_v} \Leftrightarrow x_k.type = c_C \tag{38}$$

6.4. Load Capacitor

Function: The load capacitor $c_{L,k}$ represents the capacitive load the op-amp is able to drive in its application.

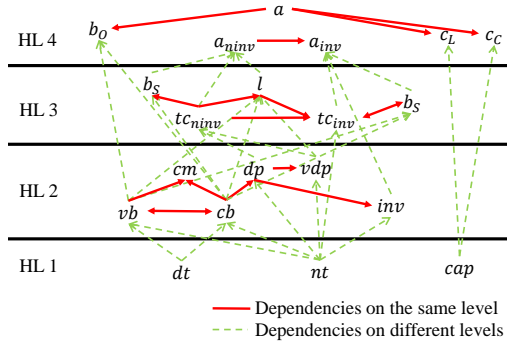


Figure 15: Dependency graph of the functional blocks in op-amps (see Fig. 1)

Structure: A load capacitor $c_{L,k}$ is connected between an output of the highest (n -th) amplification stage a_n and ground:

$$x_k = \{cap_k\} \wedge cap_k.p_1 \leftrightarrow a_n.out_j \wedge net(cap_k.p_2) = GND \Leftrightarrow x_k.type = c_L \quad (39)$$

7. Functional Block Analysis

The functional block analysis recognizes all functional blocks in an op-amp netlist based on the definitions given in Sec. 3 - 6. Fig. 15 shows the dependency graph that arises from these definitions. Note, that bidirectional dependencies exist. Therefore complex algorithms are required for the functional block analysis.

7.1. Hierarchy Level 1

On hierarchy level 1, the definitions of the functional block types are independent of each other. Therefore, the definitions given in Sec. 3 can be used for recognition without any restriction to their order.

7.2. Hierarchy Level 2

On level 2, every recognition of a functional block type depends on another functional block on the same level (10) - (18). Voltage bias and current bias are

Algorithm 1 Recognition of functional block types on hierarchy level 2

Require: $\mathcal{X} = \mathcal{X}_{nt} \cup \mathcal{X}_{dt} \cup \mathcal{X}_{dt}$
 1: $\mathcal{X}_{vb} := \{\}$ //At the beginning the set of voltage biases is empty
 2: $\mathcal{X}_{cb} := \{\}$ //At the beginning the set of current biases is empty
 3: $\mathcal{X}_{ts_n} := \text{findAllTransistorStacksNMOS}(\mathcal{X})$ //Definition (9)
 4: $\mathcal{X}_{ts_p} := \text{findAllTransistorStacksPMOS}(\mathcal{X})$ //Definition (9)
 5: **repeat**
 6: **for all** $ts_k \in [\mathcal{X}_{ts_j} |_{j \in \{n,p\}} \setminus (\mathcal{X}_{vb} \cup \mathcal{X}_{cb})]$ **do**
 7: **if** $\exists ts_l \in \mathcal{X}_{ts_j} [ts_k.d \leftrightarrow ts_l.g_m \wedge \forall ts_k.g_v [ts_k.g_v \leftrightarrow ts_l.g_w]]$ **then**
 8: **if** $\forall ts_l.g_m [ts_l.g_m \leftrightarrow (ts_k.g_m \vee ts_k.d)] \wedge$
 $\nexists ts_i \in \mathcal{X}_{ts_j} [ts_i.g_n \leftrightarrow ts_l.d]$ **then**
 9: $\mathcal{X}_{vb} := \mathcal{X}_{vb} \cup \{ts_k\}$
 10: $\mathcal{X}_{cb} := \mathcal{X}_{cb} \cup \{ts_l\}$
 11: **else if** $ts_l \in \mathcal{X}_{cb}$ **then**
 12: $\mathcal{X}_{vb} := \mathcal{X}_{vb} \cup \{ts_k\}$
 13: **end if**
 14: **end if**
 15: **end for**
 16: **until** no new voltage or current bias was found
 17: $\mathcal{X}_{cm} := \text{findAllCurrentMirrors}(\mathcal{X}_{vb}, \mathcal{X}_{cb})$ //Definition (12)
 18: $\mathcal{X}_{dp}, \mathcal{X}_{vdp} := \text{findAllDifferentialPairs}(\mathcal{X}_{nt}, \mathcal{X}_{cb})$ //Definitions (13), (15)
 19: $\mathcal{X}_{inv} := \text{findAllAnalogInverters}(\mathcal{X}_{ts_n}, \mathcal{X}_{ts_p})$ //Definition (18)
 20: $\mathcal{X} := \mathcal{X} \cup \mathcal{X}_{vb} \cup \mathcal{X}_{cb} \cup \mathcal{X}_{cm} \cup \mathcal{X}_{dp} \cup \mathcal{X}_{vdp} \cup \mathcal{X}_{inv}$
 21: $\mathcal{X} := \text{deleteIrrelevantStructures}(\mathcal{X})$ //Definition (19)
 22: **return** \mathcal{X}

at the starting point of the dependency graph being bidirectionally dependent.

240 Alg. 1 presents the recognition algorithm.

To resolve all dependencies, we propose to start with the recognition of transistor stacks (9), which are auxiliary blocks independent of all functional block types of level 2. On basis of the recognized transistor stacks, the current and voltage biases are recognized. For every substrate type, a set of transistor stacks $\mathcal{X}_{ts_j} |_{j \in \{n,p\}}$ is created (Line 3, 4). The algorithm iterates over both sets. It searches for two transistor stacks ts_k, ts_l , which are connected at their gates and also have a drain-gate connection $ts_k.d \leftrightarrow ts_l.g_m$ (Line 7). This corresponds to the definition of a voltage bias (10), taking ts_k as voltage bias connected to a current bias ts_l . It is checked if ts_l has all the gate-drain and gate-gate connections to ts_k needed for a current bias (Line 8), and if it is not connected with its drain to any gate of a transistor stack in \mathcal{X}_{ts_j} . This corresponds to the definition of a current bias (11). If this is the case, the ts_k and ts_l are *primary*

voltage and current biases, i.e., they have all gate-gate and gate-drain connection to each other. Another case is that ts_l is an already identified current bias (Line 11). In this case, the primary voltage and current bias were already recognized
 255 and a *secondary voltage bias* ts_k is recognized, e.g. a voltage bias which biases the uppermost gate of a wide-swing cascode current mirror. Note, that the last part of the voltage bias definition (10) is not checked as this is always ensured by using an valid op-amp topology.

260 The repetitive iteration over all recognized transistor stacks is needed to ensure that all secondary voltage biases are found. After finding all voltage and current biases. The current mirrors and differential pairs are found using their definitions. The analog inverter is the last functional block of HL 2, which is recognized to omit their false recognition in differential pairs. With (19) all
 265 irrelevant functional blocks are deleted from the set of all functional blocks.

7.3. Hierarchy Level 3 - 4

We combine the recognition of the functional block types of HL 3 and HL 4 as this simplifies the recognition process and resolves the bidirectional dependency of the inverting transconductance tc_{inv} and its stage bias b_s . The algorithm
 270 (Alg. 2) starts by recognizing all non-inverting transconductances. They are the only functional blocks on HL 3 that are independent of any other functional block (30).

In the next step, the loads are recognized. Here we propose not to use the exact definition of the load (24) but instead use the algorithm shown in Alg. 3.
 275 The advantage of this algorithm is that it does not depend on recognized voltage or current biases as the definition (25) does. Often external voltage biases are used to bias the load. In this case, current biases as load are not recognized. Alg. 3 is more general and uses transistor stacks for recognition. It first searches for the nets, to which the load parts are connected (Line 4 - 9). This is either
 280 the drain net of a gate connected couple $gcc_l.d$ or if no gcc_l exists, the drain nets of differential pairs in $tc_{inv,k}$. At these nets, the algorithm searches for the transistor stacks forming the load (Line 12 - 19). Note, that a gate connected

Algorithm 2 Recognition of functional block types on the hierarchy levels 3-4

Require: \mathcal{X}

```

1: //Searching for non-inverting stages
2:  $\mathcal{X}_{tc_{ninv}} := \text{findAllNonInvertingTransconductance}(\mathcal{X}_{dp}, \mathcal{X}_{vdp})$  //Definitions (20),
   (21), (22)
3:  $\mathcal{X}_l := \text{findAllLoads}(\mathcal{X}_{tc_{ninv}}, \mathcal{X})$  //Algorithm 3,
4:  $\mathcal{X}_{b_{s,ninv}} := \text{findStageBiases}(\mathcal{X}_{tc_{ninv}}, \mathcal{X}_{cb})$  //Definition (29)
5:  $\mathcal{X}_{a_{ninv}} := \text{findAllNonInvertingStages}(\mathcal{X}_{tc_{ninv}}, \mathcal{X}_l, \mathcal{X}_{b_{s,ninv}})$  //Definitions (31), (32),
   (33)
6:  $\mathcal{X} := \mathcal{X} \cup \mathcal{X}_{tc_{ninv}} \cup \mathcal{X}_l \cup \mathcal{X}_{b_{s,ninv}} \cup \mathcal{X}_{a_{ninv}}$ 
7: //Searching for inverting stages
8:  $\mathcal{X}_{ainv} = \{\}$ 
9: repeat
10:  for all  $inv_k \in \mathcal{X}_{inv}$  do
11:    if  $\exists_{ts_{k,1} \in inv_k} [\exists_{a_i \in \mathcal{X}_a} a_i.out_j \leftrightarrow ts_{k,1}.g_1] \wedge \exists_{ts_{k,2} \in inv_k} (ts_{k,2}.type = cb)$  then
12:       $tc_{inv,k} = ts_{k,1}$ 
13:       $b_{s,inv,k} = ts_{k,2}$ 
14:       $a_{inv,k} = \{tc_{inv,k}, b_{s,inv,k}\}$ 
15:       $\mathcal{X} := \mathcal{X} \cup \{tc_{inv,k}, b_{s,inv,k}, a_{inv,k}\}$ 
16:    end if
17:    if  $|\mathcal{X}_{a_{inv}}| = 1 \wedge \exists_{a_1} [a_1.type = a_s \wedge \exists_{l_1 \in a_1} [|l_1| = 1 \wedge \exists_{l_{1,1} \in l_1} (\{vb_{l,1}, vbl_2 \subseteq l_{1,1}\})]]$ 
      then
18:      if  $\exists_{ts_i} [ts_i.g_1 \leftrightarrow (vb_{l,1}.g_1 \vee vb_{l,2}.g_1) \wedge ts_i.d \leftrightarrow vb_j.d \wedge (vb_j.g_q \leftrightarrow$ 
         $a_{inv,1}.g_q |_{a_{inv,1} \in \mathcal{X}_{a_{inv}}}) |_{q \leq |vb_j|}]$  then
19:         $tc_{inv,i} = ts_i$ 
20:         $b_{s,inv,v} = vb_j$ 
21:         $a_{inv,v} = \{tc_{inv,i}, b_{s,inv,v}\}$ 
22:         $\mathcal{X} := \mathcal{X} \cup \{tc_{inv,i}, b_{s,inv,v}, a_{inv,v}\}$ 
23:      end if
24:    end if
25:  end for
26: until no new stage is found
27:  $\mathcal{X}_{b_O} := \text{findCircuitBias}(\mathcal{X}_{cb} \cup \mathcal{X}_{vb}, \mathcal{X}_a)$  //Definition (37)
28:  $\mathcal{X}_{c_C} := \text{findCompensationCapacitors}(\mathcal{X}_{cap}, \mathcal{X}_a)$  //Definition (38)
29:  $\mathcal{X}_{c_L} := \text{findLoadCapacitors}(\mathcal{X}_{cap}, \mathcal{X}_a)$  //Definition (39)
30:  $\mathcal{X} := \mathcal{X} \cup \mathcal{X}_{b_O} \cup \mathcal{X}_{c_C} \cup \mathcal{X}_{c_L}$ 
31: return  $\mathcal{X}$ 

```

Algorithm 3 findAllLoads($\mathcal{X}_{tc_{inv}}$, \mathcal{X})

Require: $\mathcal{X}_{tc_{inv}}$, \mathcal{X}

```
1:  $\mathcal{X}_i := \{\}$ 
2: for all  $tc_{inv,k} \in \mathcal{X}_{tc_{inv}}$  do
3:    $\mathcal{N} := \{\}$  // Set of nets the load parts are connected to is empty
4:   if  $\exists_{dpi \in tc_{inv,k}} \{dpi\} \subset vdp_i$  then
5:      $gcc_i = vdp_i \setminus \{dpi\}$ 
6:      $\mathcal{N} := \mathcal{N} \cup \{\text{net}(gcc_i.d_1), \text{net}(gcc_i.d_2)\}$ 
7:   else
8:      $\mathcal{N} := \mathcal{N} \cup \{\text{net}(tc_{inv,k}.out_1), \text{net}(tc_{inv,k}.out_2), \dots\}$ 
9:   end if
10:   $l_{p,n} := \{\}$  // The load part containing NMOS transistors is empty
11:   $l_{p,p} := \{\}$  // The load part containing PMOS transistors is empty
12:  for all  $n_j \in \mathcal{N}$  do
13:    if  $\exists_{ts_m} [ts_m.\Phi = \Phi_n \wedge \text{net}(ts_m.d) = n_j \wedge [ts_m.s \leftrightarrow (GND \vee tc_{inv,k}.out_z)]]$ 
14:      then
15:         $l_{p,n} := l_{p,n} \cup \{ts_m\}$ 
16:      end if
17:      if  $\exists_{ts_n} [ts_n.\Phi = \Phi_p \wedge \text{net}(ts_n.d) = n_j \wedge [ts_n.s \leftrightarrow (VDD \vee tc_{inv,k}.out_z)]]$  then
18:         $l_{p,p} := l_{p,p} \cup \{ts_n\}$ 
19:      end if
20:     $\mathcal{X}_i := \mathcal{X}_i \cup \{l_{p,p}, l_{p,n}\}$ 
21:  end for
22: return  $\mathcal{X}_i$ 
```

couple if recognized, is part of a load while a differential pair is not.

After the recognition of the loads, the stage biases of non-inverting stages
285 are recognized by definition (29). With the non-inverting transconductances,
loads and stage biases, the non-inverting stages are recognized.

In the next step, inverting stages are recognized. For recognition, we use that
an inverting stage is also a functional block of type analog inverter iff its stage
bias is of type current bias (35). This resolves the bidirectional dependency of an
290 inverting transconductance $tc_{inv,k}$ and its bias $b_{s,inv,k}$. The algorithm iterates
over all recognized analog inverters. For every analog inverter, it is checked, if
one of its stacks $ts_{k,1}$ is connected with its first gate $ts_{k,1}.g_1$ to the output of an
already recognized stage a_i . This corresponds to the definition of an inverting
transconductance $tc_{inv,k}$ (23). The output of a stage is either the output of its
295 load or the output of its transconductance (Fig. 11). The other transistor stack
 $ts_{k,2}$ in the analog inverter must be of type current bias and thus is the stage

bias (29) of the inverting stage.

After finding the first inverting stage with current bias as stage bias, it is searched for an inverting stage with voltage bias as stage bias (36). This type of
300 inverting stage is only part of an op-amp if the first stage fulfills the criteria of a symmetrical op-amp (Line 17). It is sufficient to search for a transistor stack ts_i connected with its gate $ts_i.g_1$ to one of the voltage biases in the first stage load. ts_i must be connected with its drain $ts_i.d$ to a voltage bias drain $vb_j.d$. The voltage bias vb_j must be connected with its gates to the current bias of the
305 already recognized inverting stage $a_{inv,1}$.

As inverting stages might be connected to other inverting stages, as, e.g., a third stage, it is repeatedly iterated over the set of analog inverters until no new stage is found. Thus, also multi-stage op-amps are supported by this method. Multi-stage op-amps usually comprise multiple inverting stage. Some
310 of them may be connected in frequency compensation in feedback loops [36, 37]. However, as they have the characteristic structure of an inverter and as the gate of one of the transistors in the transconductance is connected to the output of the previous stage, they are unambiguously identifiable.

After finding all amplification stages of an op-amp, the circuit bias, compen-
315 sation and load capacitors are recognized using their definitions.

8. Experimental results

In this section, we present experimental results of the functional block analysis. We illustrate the behavior of the algorithms presented in Sec. 7 on the example of a telescopic two-stage op-amp (Fig. 16). Furthermore, we discuss the
320 results of the functional block analysis on three different circuits: a symmetrical op-amp (Fig. 2), a folded-cascode op-amp with CMFB (Fig. 17) and a three-stage op-amp (Fig. 18). Overall more than 4000 different op-amp topologies have been successfully analyzed.

The computational cost of the algorithm is very low. The runtime for every
325 topology is in the area of milliseconds. The time needed to add a new functional

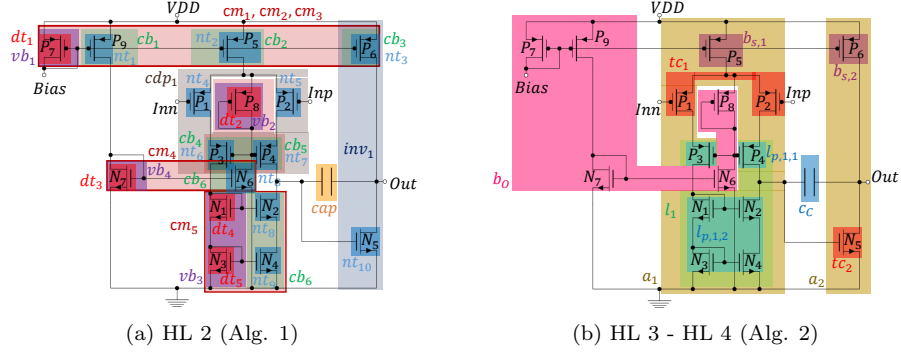


Figure 16: Blocks recognized during functional block analysis in a telescopic two-stage op-amp

block to the algorithm depends on the uniqueness of its structures. It is very low and in the area of a few hours, if many of the already implemented functional blocks are reused. More advanced functional blocks need a day integration time. Frequency compensation methods as described in [38, 39] can be integrated in this method in less than a work day.

330

Telescopic op-amp (HL 2): Fig. 16a shows all functional blocks recognized on level 2 with Alg. 1. Alg. 1 first searches for all transistor stacks in the circuit sorted according to their substrate type. All transistor stacks are marked in dark blue. Transistor stacks including transistors of the differential pair (P_1, P_2) are not shown as they are not valid (Sec. 4.6). Every transistor in the circuit is a transistor stack by itself. That means for the three transistor stacks consisting of two transistors, every transistor in these stacks is also a transistor stack by itself. The algorithm checks which of the transistor stacks are voltage and current biases. Note that, for P_5, P_8 , the transistor stacks of the individual transistors are classified as a current bias and voltage bias, respectively. P_5 has a gate connection to the voltage bias $vb_1(P_7)$ and therefore fulfills the definition of a current bias. P_8 has a gate-drain connection to itself and therefore is a voltage bias connected with its gate to the gates of the current biases $cb_4(P_3)$ and $cb_5(P_5)$. The other two transistor stacks N_1, N_3 and N_2, N_4 , form a current mirror. The transistor stacks of the individual transistors therefore are irrelevant.

340

345

Note that vb_2 does not form current mirrors with cb_4 and cb_5 as their sources are not connected to the same net. All voltage and current biases in this circuit are primary. All voltage biases have their needed gate-drain connection (10) by themselves, such that no secondary voltage biases are needed to establish a drain-gate connection of a voltage bias gate. Alg. 1 ends with the recognition
 350 of the cascode differential pair cdp_1 (17) and the analog inverter inv_1 (18).

Telescopic op-amp (HL 3 - HL 4): Fig. 16b shows all functional blocks recognized on levels 3 and 4 with Alg. 2. The algorithm first recognizes the differential pair as simple non inverting first stage transconductance tc_1 . For
 355 the load recognition, the drain nets of P_3, P_4 are used. P_3, P_4 form the gate connected couple part of the cascode differential pair cdp_1 . Two load parts are found: The gate connected couple forms the load part with p-doping. The load part with n-doping consists of the current mirror $cm_5 = \{ts_{n,1}, ts_{n,2}\}$. As stage bias, the current bias cb_2 is found as it is connected with its drain to the source
 360 of tc_1 . With it, all parts of the non-inverting first stage a_1 are recognized. In the next step, Alg. 2 checks if the inverter recognized on level 2 is a second stage. This is true, as P_6 was recognized as current bias cb_3 and $ts_{n,3}(N_5)$ is connected with its gate to one output of the first stage. Because the first stage does not fulfill the criteria of a symmetrical op-amp, it is not searched for an inverting
 365 stage with voltage bias as stage bias. The voltage and current biases not part of the two amplification stages are recognized as circuit bias b_O . The recognition ends by identifying the capacitor in the circuit as compensation capacitor.

Symmetrical op-amp with an additional inverting stage: Fig. 2 shows the results of the functional block analysis for a symmetrical op-amp with an additional
 370 inverting stage a_3 . During the recognition of the inverting stages, first inv_2 is recognized as inverting second stage $a_{2,1}$. Afterwards $a_{2,2}$ is recognized, a_1 fulfills the condition of a first stage of a symmetrical op-amp and with $a_{2,1}$, the needed second stage with current bias as stage bias is given (36). The transistor stack $\{nt_4(P_3), nt_6(P_5)\}$ fulfills the definition of a non-inverting transconductance $tc_{2,2}$ (23). vb_2 is the stage bias with voltage output. The gate-gate
 375 connection to the stage bias of $a_{2,1}$ is given. Note, that for a correct identifica-

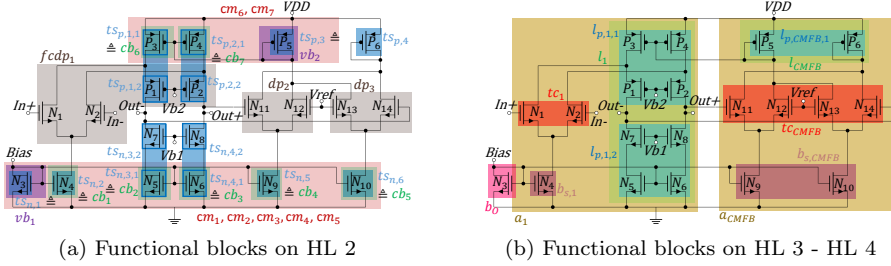


Figure 17: Folded-cascode op-amp with CMFB

tion of a_3 the exact definition of an inverting stage must be used (34). As P_7 has a gate connection to one output of the first stage, a drain of the differential pair, it is considered as possible inverting transconductance of another second stage. As for this transconductance, no stage bias exist because N_6 is not of type bias, it is not recognized as transconductance. Instead, after $a_{2,1}$ is recognized, N_6 is identified as inverting transconductance, because it has a connection to an output of $tc_{2,2}$. P_7 is its stage bias.

Folded-cascode op-amp with CMFB: Fig. 17 shows the results of the functional block analysis in a folded-cascode op-amp with CMFB. The four load transistors P_1, P_2, N_7, N_8 are externally biased by the pins $Vb1$ and $Vb2$ respectively. Hence, these four transistors are not recognized as current biases (Fig. 17a) as they are not connected with their gates to a voltage bias. However with Alg. 3, they are still recognized as part of the load (Fig. 17b). P_6 is also neither identified as current nor voltage bias as it does not have any gate-gate connections to a another transistor with same doping. However, it fulfills the functional definition of a load as it has a drain-drain connection to tc_{CMFB} . Therefore, it is recognized with Alg. 3 correctly even if it does not fulfill the definition of a load entirely (24).

Three-stage op-amp: Fig. 18 shows the results of the analysis for a three-stage op-amp. Two analog inverters inv_1, inv_2 are recognized on HL 2 (Fig. 18a). One of the transistors N_5 (inv_1), P_7 (inv_2) is identified to be part of a current mirror. The other transistor P_6 (inv_1), N_6 (inv_2) is not part of any

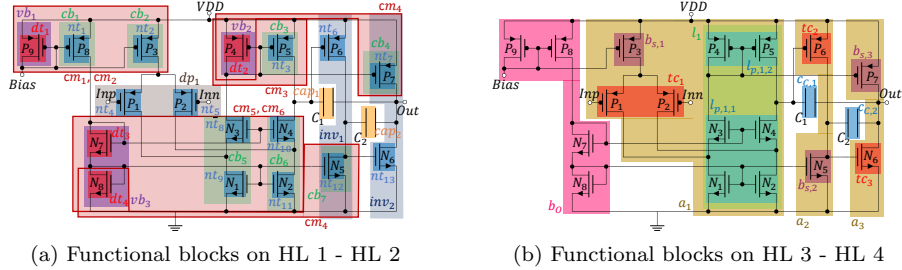


Figure 18: Three-stage op-amp

additional functional block on HL 2. After recognizing the first and second
 400 stage with Alg. 2, the third stage is recognized (Fig. 18b). With the gate of N_6
 connected to the drain of N_5 , the input of third stage is connected to the output
 of the second stage (34). P_7 is a identified current bias. Hence, inv_2 fulfills all
 criteria of a third stage. Alg. 2 ends by identifying the compensation capacitors
 $c_{c,1}, c_{c,2}$. Both capacitors a connected between the output of two stages, $c_{c,1}$
 405 between the output of first and third stage, $c_{c,2}$ between second and third stage.
 Hence, both capacitors fulfill (38).

9. Application of the Hierarchical Functional Block Decomposition Method

Two applications of the functional block decomposition method are pre-
 410 sented: A sizing method (Sec. 9.1, details in [2]) and a structural synthesis
 method (Sec. 9.2, details in [3]).

9.1. Application to Circuit Sizing

The common manual design process is based on analytical equations as de-
 scribed in [17, 18, 19, 20, 21]. For each functional block described in Secs. 3 -
 6, a behavior model can be derived based on these standard equations resulting
 in a hierarchical performance equation library (HPEL) [2]. For the functional
 blocks on HL 3, the equations part of the library describe, e.g., the input and

output conductance ($gin_{fb_k}, gout_{fb_k}$) of a functional block fb_k . Following equation for instance holds for the output conductance $gout_{fb_k}$ of a functional block consisting of one or two transistor stacks ts_k :

$$gout_i = \begin{cases} gd_{t_{k,out}}, & \{t_{k,out}\} = ts_k \subseteq fb_k \\ \frac{gd_{t_{k,out}}gd_{t_{k,supply}}}{gm_{t_{k,out}}}, & \{t_{k,out}, t_{k,supply}\} = ts_k \subseteq fb_k \end{cases} \quad (40)$$

$gd_{t_{k,j}}, gm_{t_{k,j}}$ are the output und input conductance of a transistor in fb_k with j giving the position of the transistor in the transistor stack. There are exceptions
415 to this equation which are discussed in [2].

An equation for the output resistance $R_{out,n}$ of an amplification stage functional block a_n on HL 4 is developed based on (40) and the m functional blocks of the stage connected to the output net of the stage. These functional blocks can be stage biases, load parts and transconductances.

$$R_{out,n} = \frac{1}{\sum_{j=1}^m gout_{fb_j}} \quad (41)$$

This equation is part of the equation describing the open-loop gain of a stage $A_{D,n}$ which is on the same hierarchy level in the HPEL:

$$A_{D,n} = gin_n \cdot R_{out,n}; \quad A_{D,0} = \prod_{n=1}^l A_{D,n} \quad (42)$$

with gin_n the input conductance of the stage. The open-loop gain equation of the overall op-amp $A_{D,0}$ is part of HL 5 of the HPEL. l is the number of all stages in the op-amp,

Analogously, performance equations for all functional blocks that have been
420 presented in Sec. 3 - Sec. 6 have been established [2]. After a functional block analysis of a given op-amp topology according to the methods presented in the paper, the corresponding performance equations of the functional blocks are automatically composed forming a behavioral model of the op-amp performance. This model forms a Mixed-Integer Non-linear Programming problem (MINLP)

Table 1: Results of the sizing method for the telescopic op-amp Fig. 16

(a) Performance values; M: sizing method; S: simulation

Constraints	Spec.	M	S
Gate-area ($10^3 \mu\text{m}^2$)	≤ 15	5.8	-
Quiescent power (mW)	≤ 10	5.8	6.1
Max. common-mode input voltage (V)	≥ 3	3.3	4.4
Min. common-mode input voltage (V)	≤ 2	0	0.1
Max. output voltage (V)	≥ 4	4.5	4.5
Min. output voltage (V)	≤ 1	0.3	0.2
CMRR (dB)	≥ 90	130	146
Unity-gain bandwidth (MHz)	≥ 7	10	7
Open-loop gain (dB)	≥ 80	120	93
Slew rate ($\frac{\text{V}}{\mu\text{s}}$)	≥ 15	28	22
Phase Margin ($^\circ$)	≥ 60	60	67

(b) Device sizes

Variable	Value ($\mu\text{m}/\text{pF}$)
$W_{P_{1,2}}; L_{P_{1,2}}$	172;9
$W_{P_{3,4}}; L_{P_{3,4}}$	27;4
$W_{P_5}; L_{P_5}$	247;3
$W_{P_6}; L_{P_6}$	515;3
$W_{P_7}; L_{P_7}$	7;3
$W_{P_8}; L_{P_8}$	7;4
$W_{P_9}; L_{P_9}$	43;3
$W_{N_{1,2}}; L_{N_{1,2}}$	90;1
$W_{N_{3,4}}; L_{N_{3,4}}$	90;1
$W_{N_5}; L_{N_5}$	130;1
$W_{N_6}; L_{N_6}$	269;1
$W_{N_7}; L_{N_7}$	166;9
C_c	6.4

425 for sizing the circuit, which is solved, e.g., with a constraint programming approach [40].

Table 1 shows the results of the sizing method for the telescopic op-amp (Fig. 16) using the specifications given in column 2 of Table Ia. The values calculated with the analytical equations within the sizing method are compared
 430 to simulation results using a BSIM3v3 models. The deviations due to the simpler transistor model are less than 30% and within designer expectations.

9.2. Application to Structural Synthesis

The functional block library (Sec. 3 - Sec. 6) can be applied to structural synthesis by functional block composition. Alg. 4 gives an algorithm to create
 435 the structural implementations S_{new} of a functional block fb_{new} based on the implementation S_1, \dots, S_i of its subblocks and a set of characteristic connections R_c . The two-transistor implementations of a current bias (Fig. 5), e.g., are created based on two structural implementation sets S_1, S_2 containing normal and diode transistors of the same doping Φ ($S_1 : NT_\Phi, DT_\Phi$; $S_2 : NT_\Phi$). Every
 440 combination of $s_1 \in S_1, s_2 \in S_2$ has a drain-source connection ($R_c : s_1.d \leftrightarrow s_2.s$). Thus, all structural implementations of a two-transistor current bias are created. More complex functional blocks need additional rules set as explained in [3].

Algorithm 4 Synthesis of a functional block

Require: Set of subblock implementations S_1, \dots, S_i ; Connection rules R_c

```
1:  $S_{new} := \{ \}$  //The set of structural implementations of  $fb_{new}$  is empty
2: for all  $s_1 \in S_1$  do
3:   ...
4:   for all  $s_i \in S_i$  do
5:      $s_{new} := \text{createNewImplementation}(s_1, \dots, s_i, R_c)$ 
6:      $S_{new} := S_{new} \cup \{s_{new}\}$ 
7:   end for
8:   ...
9: end for
10: return  $S_{new}$ 
```

Table 2: Amplification stage composition of the resulting topologies for the specification in Table Ia

First stage type	simple		folded-cascode		telescopic		symmetrical	total
# stages	1	2	1	2	1	2	-	
# topologies	0	111	0	181	20	77	58	447

With Alg. 4, the structural implementations of all functional blocks in Secs. 3
445 - 6 are created allowing a creation of up to 3000 topologies. The corresponding
composition graph is presented in [3]. For given specifications, the topologies are
sized and evaluated using an enhanced version of the sizing method described in
Sec. 9.1. The respective algorithm is presented in [3]. Table 2 shows the output
of the synthesis tool for the specifications in Table Ia. As the specifications are
450 not highly demanding and no upper bounds are specified, many topologies are
able to fulfill the specifications, e.g. the telescopic op-amp in Fig. 16. Defining
more strict specifications reduces the number of created topologies significantly.

10. Conclusion and Outlook

This paper presented a new method to represent op-amps by their functional
455 block. The functional blocks are ordered hierarchically. For each functional
block, a systematic functional and structural description is given allowing an
automatic recognition. Two different areas of applications are presented: To-
gether with a performance equation library, the functional block analysis al-
lows a topology-independent sizing of op-amps. A functional block composition
460 method allows structural synthesis of op-amps. Thousands of different op-amp

topologies are created based on hierarchically generated functional blocks by small rule sets.

Future work remains in including more feedback compensation techniques in the method. Currently, a compensation capacitor is supported in the recognition
465 algorithm. For multi-stage op-amps, additional compensation circuits as, e.g., [38, 39] are needed. As they have a fixed structure, the compensation circuits can be added to the method. Future research will also be on including the functional block composition method in layout synthesis.

References

- 470 [1] G. Shi, Automatic stage-form circuit reduction for multistage opamp design equation generation, *ACM Transactions on Design Automation of Electronic Systems* (Oct. 2019). doi:10.1145/3363499.
- [2] I. Abel, M. Neuner, H. Graeb.
- [3] I. Abel, H. Graeb, Structure Synthesis of Basic Op-Amps by Functional
475 Block Composition, .
URL <http://arxiv.org/abs/2101.07517>
- [4] M. d. Hershenson, S. P. Boyd, T. H. Lee, Optimal design of a CMOS op-amp via geometric programming, *IEEE Transactions on Computer-Aided Design of Integrated Circuits and Systems* (2001).
- 480 [5] P. C. Maulik, L. R. Carley, R. A. Rutenbar, Integer programming based topology selection of cell-level analog circuits, *IEEE Transactions on Computer-Aided Design of Integrated Circuits and Systems* (1995).
- [6] A. Gerlach, J. Scheible, T. Rosahl, F. Eitrich, A generic topology selection method for analog circuits with embedded circuit sizing demonstrated on
485 the OTA example, in: *Design, Automation Test in Europe Conference Exhibition*, 2017.

- [7] A. Graupner, R. Jancke, R. Wittmann, Generator based approach for analog circuit and layout design and optimization, in: Design, Automation Test in Europe, 2011.
- 490 [8] A. Das, R. Vemuri, A graph grammar based approach to automated multi-objective analog circuit design, in: Design, Automation Test in Europe Conference Exhibition, 2009.
- [9] T. McConaghy, P. Palmers, M. Steyaert, G. G. E. Gielen, Trustworthy genetic programming-based synthesis of analog circuit topologies using hierarchical domain-specific building blocks, IEEE Transactions on Evolutionary
495 Computation (2011).
- [10] H. Graeb, S. Zizala, J. Eckmueller, K. Antreich, The sizing rules method for analog integrated circuit design, in: IEEE/ACM International Conference on Computer Aided Design, 2001.
- 500 [11] T. Massier, H. Graeb, U. Schlichtmann, The Sizing Rules Method for CMOS and Bipolar Analog Integrated Circuit Synthesis, IEEE Transactions on Computer-Aided Design of Integrated Circuits and Systems (2008).
- [12] M. Meissner, L. Hedrich, FEATS: Framework for Explorative Analog Topology Synthesis, IEEE Transactions on Computer-Aided Design of Integrated
505 Circuits and Systems (2015).
- [13] Z. Zhao, L. Zhang, An Automated Topology Synthesis Framework for Analog Integrated Circuits, IEEE Transactions on Computer-Aided Design of Integrated Circuits and Systems (2020).
- [14] M. Eick, H. Graeb, MARS: Matching-Driven Analog Sizing, IEEE Transactions on Computer-Aided Design of Integrated Circuits and Systems (2012).
510
- [15] H. Li, F. Jiao, A. Daboli, Analog circuit topological feature extraction with unsupervised learning of new sub-structures, in: Design, Automation Test in Europe Conference Exhibition, 2016.

- [16] M. Neuner, I. Abel, H. Graeb, Library-free structure recognition for analog
515 circuits, in: Design, Automation Test in Europe Conference Exhibition,
2021.
- [17] D. R. H. Phillip E. Allan, CMOS Analog Circuit Design, Oxford University
Press, 2012.
- [18] K. R. Laker, W. M. C. Sansen, Design of analog integrated circuits and
520 systems, McGraw-Hill, 1994.
- [19] W. M. C. Sansen, Analog Design Essentials, Springer, 2007.
- [20] D. Johns, K. Martin, Analog Integrated Circuit Design, John Wiley and
Sons, 1997.
- [21] P. R. Gray, R. G. Meyer, P. J. Hurst, S. H. Lewis, Analysis and Design of
525 Analog Integrated Circuits, 4th Edition, John Wiley & Sons, Inc., USA,
2001.
- [22] M. G. R. Degrauwe, O. Nys, E. Dijkstra, J. Rijmenants, S. Bitz, B. L. A. G.
Goffart, E. A. Vittoz, S. Cserveny, C. Meixenberger, G. van der Stappen,
H. J. Oguey, IDAC: An interactive design tool for analog CMOS circuits,
530 IEEE Journal of Solid-State Circuits (1987).
- [23] F. El-Turky, E. Perry, BLADES: An artificial intelligence approach to ana-
log circuit design, IEEE Transactions on Computer-Aided Design of Inte-
grated Circuits and Systems (1989).
- [24] R. Harjani, R. A. Rutenbar, L. Carley, OASYS: A Framework for Ana-
535 log Circuit Synthesis, IEEE Transactions on Computer-Aided Design of
Integrated Circuits and Systems (1989).
- [25] H. Y. Koh, C. H. Sequin, P. R. Gray, OPASYN: a compiler for CMOS
operational amplifiers, IEEE Transactions on Computer-Aided Design of
Integrated Circuits and Systems (1990).

- 540 [26] G. Van der Plas, G. Debyser, F. Leyn, K. Lampaert, J. Vandenbussche, G. Gielen, W. Sansen, P. Veselinovic, D. Leenaerts, AMGIE–A Synthesis Environment for CMOS Analog Integrated Circuits, *IEEE Transactions on Computer-Aided Design of Integrated Circuits and Systems* (2001).
- [27] K. Antreich, H. Graeb, C. Wieser, Circuit analysis and optimization driven
545 by worst-case distances, *IEEE Transactions on Computer-Aided Design of Integrated Circuits and Systems* (1994).
- [28] E. S. Ochotta, R. A. Rutenbar, L. R. Carley, Synthesis of High-Performance Analog Circuits in ASTRX/OBLX, *IEEE Transactions on Computer-Aided Design of Integrated Circuits and Systems* (1996).
- 550 [29] B. Liu, F. V. Fernandez, G. Gielen, Efficient and Accurate Statistical Analog Yield Optimization and Variation-Aware Circuit Sizing Based on Computational Intelligence Techniques, *IEEE Transactions on Computer-Aided Design of Integrated Circuits and Systems* (2011).
- [30] G. Berkol, E. Afacan, G. Dundar, A. E. Pusane, F. Baskaya, A novel yield
555 aware multi-objective analog circuit optimization tool, in: *IEEE International Symposium on Circuits and Systems*, 2015.
- [31] F. Passos, E. Roca, J. Sieiro, R. Fiorelli, R. Castro-Lopez, J. M. Lopez-Villegas, F. V. Fernandez, A Multilevel Bottom-up Optimization Methodology for the Automated Synthesis of RF Systems, *IEEE Transactions on*
560 *Computer-Aided Design of Integrated Circuits and Systems* (2019).
- [32] A. Canelas, R. Pova, R. Martins, N. Lourenco, J. Guilherme, J. P. Carvalho, N. Horta, FUZY: A Fuzzy C-Means Analog IC Yield Optimization using Evolutionary-based Algorithms, *IEEE Transactions on Computer-Aided Design of Integrated Circuits and Systems* (2019).
- 565 [33] T. McConaghy, P. Palmers, M. Steyaert, G. G. E. Gielen, Variation-Aware Structural Synthesis of Analog Circuits via Hierarchical Building Blocks

and Structural Homotopy, *IEEE Transactions on Computer-Aided Design of Integrated Circuits and Systems* 28 (9) (2009).

- 570 [34] F. H. Bennett, M. A. Keane, D. Andre, J. R. Koza, Automatic Synthesis of the Topology and Sizing for Analog Electrical Circuits using Genetic Programming , in: EUROGEN workshop in Jyvdskyld, Finland, 1999.
- [35] C. Ferent, A. Doboli, Novel circuit topology synthesis method using circuit feature mining and symbolic comparison, in: Design, Automation Test in Europe Conference Exhibition, 2014.
- 575 [36] Ka Nang Leung, P. K. T. Mok, Analysis of multistage amplifier-frequency compensation, *IEEE Transactions on Circuits and Systems I: Fundamental Theory and Applications* 48 (9) (2001).
- [37] J. Ramos, Xiaohong Peng, M. Steyaert, W. Sansen, Three stage amplifier frequency compensation, in: ESSCIRC 2004 - 29th European Solid-State Circuits Conference, 2003.
- 580 [38] G. Palmisano, G. Palumbo, An optimized compensation strategy for two-stage cmos op amps, *IEEE Transactions on Circuits and Systems I: Fundamental Theory and Applications* 42 (3) (1995).
- [39] G. Palmisano, G. Palumbo, A compensation strategy for two-stage cmos opamps based on current buffer, *IEEE Transactions on Circuits and Systems I: Fundamental Theory and Applications* 44 (3) (1997).
- 585 [40] I. Abel, M. Neuner, H. Graeb, COPRICSI: CONstraint-PRogrammed Initial Circuit Sizing, *Integration* (2020).